JPE 9-4-13

A Solar Cell Based Coarse Sun Sensor for a Small LEO Satellite Attitude Determination

Mohamed Zahran† and Mohamed Aly*

† Electronics Research Institute, PV Dept., NRC Blg., El-tahrir St., Dokki, Egypt
†Department of Electrical Engineering, Jizan University, Jizan, Saudi Arabia
*Department of Aerospace Engineering, Old Dominion University, Norfolk, U.S.A

ABSTRACT

The sun is a useful reference direction because of its brightness relative to other astronomical objects and its relatively small apparent radius as viewed by spacecrafts near the Earth. Most satellites use solar power as a source of energy, and so need to make sure that solar panels are oriented correctly with respect to the sun. Also, some satellites have sensitive instruments that must not be exposed to direct sunlight. For all these reasons, sun sensors are important components in spacecraft attitude determination and control systems. To minimize components and structural mass, some components have multiple purposes. The solar cells will provide power and also be used as coarse sun sensors.

A coarse Sun sensor is a low-cost attitude determination sensor suitable for a wide range of space missions. The sensor measures the sun angle in two orthogonal axes. The Sun sensor measures the sun angle in both azimuth and elevation. This paper presents the development of a model to determine the attitude of a small cube-shaped satellite in space relative to the sun's direction. This sensor helps small cube-shaped Pico satellites to perform accurate attitude determination without requiring additional hardware [1].

Keywords: Sun Sensor, Attitude Determination, Space Solar Cells & Solar Array, LEO Satellite, Body Mounted SA

1. Introduction

To determine the attitude and position of a spacecraft, its orientation and location relative to some frame of reference of a well known celestial body must be defined. To accomplish this, one or more reference vectors should be chosen from which the spacecraft position and attitude can be referenced. The most commonly used vectors are unit vectors directed toward the Sun, the center of the Earth, a known star, or the magnetic field of the Earth. An attitude sensor is a mechanism which measures the orientation of these reference vectors in the spacecraft body frame of reference. By determining the orientation of two or more of these reference vectors relative to the spacecraft axes, the orientation of the spacecraft in space can be determined. Similarly, the position of a spacecraft can be determined from several reference vectors by triangulation [2].

Sun Sensors are one of the most common AD systems; these sensors determine the satellite's orientation relative

Manuscript received December 22, 2008; revised June 3, 2009
†Corresponding Author: mbazahran_2007@yahoo.com
Tel: + 9667-3230003, Fax: +9667- 3230004, Jizan University
Dept. of Electrical Eng., Jizan University, Jizan, Saudi Arabia
* Dept. of Aerospace Eng., Old Dominion Univ., Norfolk, U.S.A

to the sun by measuring the amount of light or shadow on them. There are several types of Sun Sensors; however, in this article we will focus on Analog Sun Sensors because, unlike other sensors, they use the onboard solar cells of the satellite without requiring additional hardware [1], [19-22].

Because of the advantages of Analog Sun Sensors for LEO-satellites, a technique for improving existing analog sun sensors was developed and will be presented in this paper.

2. Sensors for Attitude Determination

Sun sensors are the most commonly used attitude sensors and are flown on almost every satellite. Since most missions require solar power and have sun-sensitive equipment which needs protection against sunlight or solar heat, sun sensors are crucial to almost all spacecraft.

There are basically three types of sensors:

· Analog sun sensors (ASS),
· Sun presence sensors, and
· Digital sensors.

$$I_1(\alpha) = I_0 \cos(\alpha_0 - \alpha)$$
$$I_2(\alpha) = I_0 \cos(\alpha_0 + \alpha) \quad (1)$$

$$\Delta I = I_2 - I_1$$
$$= I_0 \cos(\alpha_0 + \alpha) - I_0 \cos(\alpha_0 - \alpha) \quad (2)$$
$$= 2I_0 \sin\alpha_0 * \sin\alpha = \sin\alpha$$

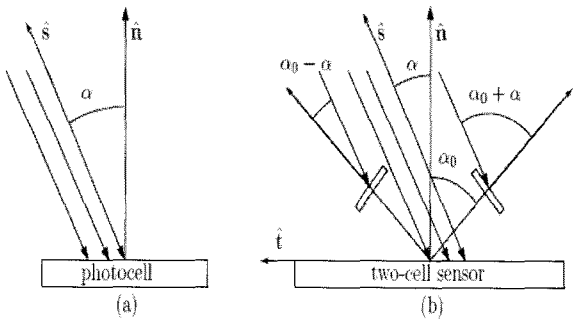

Fig. 1. Photocells for Sun Sensors. (a) Single photocell. (b) Pair of photocells for measurement of α in $\hat{n}$ - $\hat{t}$ plane.

2.1 Analog Sun Sensors (Cosine Detectors)

These sun sensors are simple flat photodiodes, embedded in the plastic of a disc. These allow a photocurrent, roughly proportional to the cosine of the angle between the normal to the photodiode and the line to the sun [3].

Analog sensors have a continuous output signal. The use of several solar cells arranged such that each gives a different output due to a given sun incidence angle will result in a sun vector orientation relative to the spacecraft body reference frame [4]. The current outputs of the solar arrays based on cosine sun detectors as described by [5]. The current varies by the incidence angle according to the function:

$$i(a) = i(o) \cos a$$

Where,

I is the measured current,
I(o) is the maximum current output, and
α is the incidence angle measured from orthogonal as shown in the following figure.

The angles are sent to an algorithm to determine a body-fixed sun vector. This is compared with the inertial sun vector.

2.2 Sun presence sensors

Sun presence detectors generate a constant output signal whenever the Sun is in their field of view (FOV). These sensors are used in two ways: one is to position the spacecraft or its experiments to protect sun sensitive areas or to use the solar energy, and another is to activate the hardware by phase angle measurement.

2.3 Digital Sun Sensors

Common digital sun sensors for spinning spacecraft are composed of two parts: the command unit and the measurement unit. The command unit basically acts as a sun presence detector, and the measurement unit puts out a digital output which is a representation of the sun incidence angle relative to the normal of the sensor face whenever the Sun is in the FOV of the command unit.

3. Analog Sun sensors applications

Sun sensors can provide a directional measurement with respect to the Sun. Additionally, Earth sensors provide a line of sight vector to the Earth. Therefore, both sets of information can be added as additional measurements to estimate the complete orbital position and velocity [6]. In the following paper, a sample of an ASS is presented.

3.1 Omni-Directional Differential Sun Sensor

Michael Swartwout et. al, have reported in [7] that, the solar panel current information and knowledge of panel geometry are used in order to create a virtual sun sensor that can roughly determine the satellite's sun angle. Fig. 2 depicts the general geometry of two body-mounted solar panels. The ideal solar panel currents produced from this configuration are as follows:

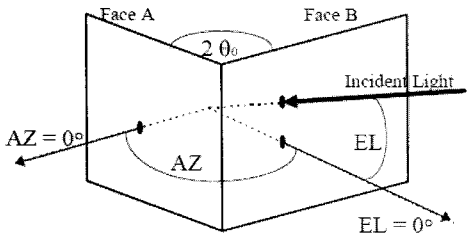

Fig. 2. General Body Mounted Solar Panel Geometry.

For the current generated on each solar panel, the following formula can be used:

$$I_A = I_{AO} \cos(AZ) \cos(EL) \tag{3}$$

$$I_B = I_{BO} \cos(AZ - 2\theta_0)\cos(EL) \tag{4}$$

Where

AZ = satellite referenced solar azimuth
EL = satellite referenced solar elevation
θ_0 = half angle between panels

The equations are differenced, manipulated, linearized, normalized, and combined in order to provide an estimated solar azimuth and solar elevation.

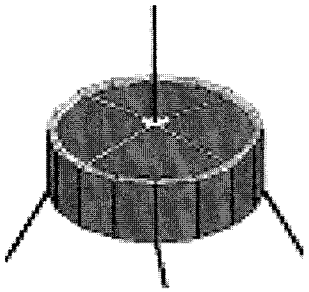

Fig. 3. IRECIN schematic view.

3.2 IRECIN Nano-satellite

M. Ferrante et. al, have reported in [8] that the IRECIN nano-satellite is a prism constituted of 16 external sides, 22 cm in width and 9.7 cm in height, weighing less than 1.5 kg.

The solar panels, made of silicon solar cells, are body mounted on all external faces. The solar panels needed for power generation are also used as a sensing system for attitude determination, eliminating the need for the sun sensor usually employed in spinning spacecraft attitude determination.

3.3 CubeSat Design

Hank Heidt et. al, have reported in [9] that the basic design of the satellite is comprised of a cube structure with a stack of circuit boards inside. Each face of the satellite will be covered with solar cells. To minimize components and structural mass, some components have multiple purposes. The solar cells will provide power and also be used as sun sensors.

4. Dynamic Modeling of Satellite Attitude

Firstly, the set of coordinates and coordinate frames in which the dynamic model will be developed have to be set. Three coordinate frames were chosen to model the dynamics of the satellite: an inertial frame, a rotating (orbital) frame, and a body fixed (also rotating) frame [10]. The inertial and rotating frames are graphically depicted in Fig. 4.

The inertial frame is labeled X-Y-Z and its origin is located at the center of the Earth with the X-axis defined to point in the direction of the Vernal Equinox, Z pointing north and Y completing the right handed frame.

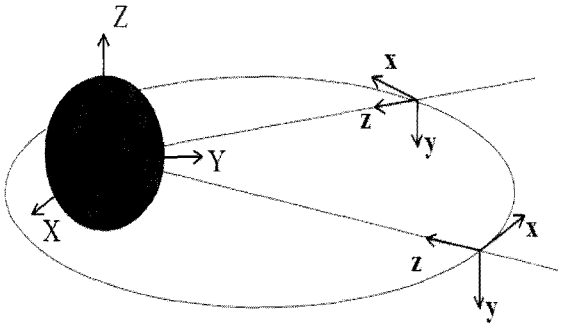

Fig. 4. The inertial and rotating frames.

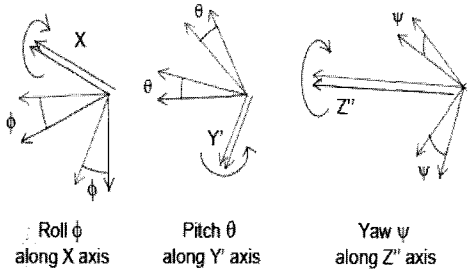

Fig. 5. Body 1-2-3 Rotation.

The Local Rotating (orbital) frame is labeled x-y-z and its origin is centered on the satellite center of mass. The x-axis points east in the plane of the orbit (flight direction), y points south perpendicular to the orbital plane, and z is nadir pointing (i.e. toward the center of the Earth). Although this frame is defined with its origin at the center of mass and rotates around the orbital plane with the satellite, it is not fixed in the body of the satellite. Therefore, the z-axis will always be nadir pointing.

The body frame is defined such that it is fixed in the body of the satellite and, thus, will be used to determine its orientation with respect to the rotating (orbital) frame.

In order to relate the rotating frame to the body frame a 1-2-3 body Euler rotation is performed. Initially, the body frame can be assumed to be aligned with the rotating frame, which is b1 aligned along the x-axis, b2 along the y-axis, and b3 along the z-axis. First, the body frame is pitched ϕ degrees about the x-axis. Next, the resulting intermediate frame is pitched θ degrees about the y-axis and, finally, yawed ψ degrees about the z-axis. These three rotations, ϕ, θ and ψ, are shown in Fig. 5 and expressed by equations (5) – (7).

$$R_x(\phi)=\begin{bmatrix}1 & 0 & 0\\ 0 & c\phi & -s\phi\\ 0 & s\phi & c\phi\end{bmatrix} \tag{5}$$

$$R_y(\theta)=\begin{bmatrix}c\theta & 0 & s\theta\\ 0 & 1 & 0\\ -s\theta & 0 & c\theta\end{bmatrix} \tag{6}$$

$$R_z(\psi)=\begin{bmatrix}c\psi & -s\psi & 0\\ s\psi & c\psi & 0\\ 0 & 0 & 1\end{bmatrix} \tag{7}$$

Combining the results of these three rotations leads to a direction cosine matrix allowing the transformation of any vector from the rotating frame to the body frame. The matrix becomes,

$$R_b^o(\Theta)=\begin{bmatrix}c\theta c\psi & c\phi s\psi + s\phi s\theta c\psi & s\phi s\psi - c\phi s\theta c\psi\\ -c\theta s\psi & c\phi c\psi - s\phi s\theta c\psi & s\phi c\psi + c\phi s\theta s\psi\\ s\theta & -s\phi c\theta & c\phi c\theta\end{bmatrix} \tag{8}$$

5. Sun Sensor modeling

The Sun provides a reference when the satellite is in line of view of it. The Suns visibility from the satellite is dependent on orbit, and during an eclipse, the reference availability ceases [11].

5.1Sensor model

In principle, the Sun sensor is a measurement of the Sun's relative position with respect to the satellite's body frame. This position, expressed as a direction by a vector, is called the Sun vector measurement, and may be modeled as

$$S^b = R_o^b S_{ref}^o + V_{sun} \tag{9}$$

Where,

R_o^b is the actual rotation matrix,

S_{ref}^o is the sun vector reference,

V_{sun} is the measurement noise.

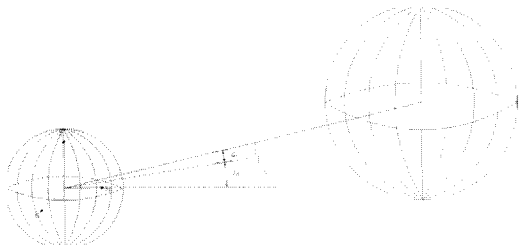

Fig. 6. Sun position relative to the Earth.

5.2 Sun reference model

In order to utilize the Sun vector measurement, knowledge of the Sun's position relative to the satellite's orbital position is needed for comparison. The reference model presented in this section is based on the work done by Wertz [4]. Here a model simplification is presented by describing the Sun-Earth related motion as seen from the Earth, i.e. the Sun revolves around the Earth as the Earth revolves around the Sun, illustrated in Fig. 6. The elevation of the Sun varies periodically through a year and is given by

$$\varepsilon_S = \frac{23\pi}{180}\sin\left(\frac{Ts}{365}2\pi\right) \tag{10}$$

Where

Ts is the time given in days, since the first day of spring.

By a period of 365 days, the Sun's orbit around the Earth is given by

$$\lambda_S = \frac{Ts}{365}2\pi \tag{11}$$

Where

λ_S is called the Sun's orbit parameter.

The Sun's position at a given time relative to the Earth-Centered Inertial (ECI) frame can now be expressed as

$$S^i_{ref} = R_y(\varepsilon_S)R_z(\lambda_s)S^i_0 \tag{12}$$

Where

$S^i_0 = [1\ 0\ 0]^T$ is the Sun's position when the Earth passes vernal equinox,

Ry and Rz are the simple rotations about the Y and Z axis by θ and ψ.

Then, the Sun's position relative to the satellite is given by:

$$S^o_{ref} = R^o_i S^i_{ref} \tag{13}$$

6. Sun Vector for cubical (body mounted) satellites

The mathematical model of a cube-shaped sun sensor that looks like a body mounted cubical satellites is given in [10].

6.1 Sun Vector in orbital frame

The derivation of the output signal of the top cell or a large solar array in the same plane (I--TC-n) is presented in [12]. In the same way, the output signal for the six sides of the cube-shaped coarse sun sensor solar cells (Fig. 8 and Fig. 9) can be expressed as shown in the six terms of Equations (14) – (19).

$$TC\_o/p_n(\tau) = \{\sin E(t)*\cos A(\tau)\}, \tag{14}$$

$$BC\_o/p_n(\tau) = -\{\sin E(t)*\cos A(\tau)\}, \tag{15}$$

$$FR\_o/p_n(\tau) = K\{\cos E(t) - \sin E(t)*\cos A(\tau)\}, \tag{16}$$

$$FL\_o/p_n(\tau) = -K\{\cos E(t) + \sin E(t)*\cos A(\tau)\}, \tag{17}$$

$$BR\_o/p_n(\tau) = K\{\cos E(t) + \sin E(t)*\cos A(\tau)\}, \tag{18}$$

$$BL\_o/p_n(\tau) = -K\{\cos E(t) - \sin E(t)*\cos A(\tau)\}, \tag{19}$$

Where:

TC	is the top cell,
BC	is the bottom cell,
FR	is the front right cell,
FL	is the front left cell,
BR	is the back right cell,
BL	is the back left cell,

A is the sun azimuth,
A = 0 - 2p, A=0 at Zenith (Solar Peak),
E is the sun elevation,
τ is the orbit time,
t is the time from launching.
K factor depends on the satellite configuration,
K = 0.707 for most cubical or body mounted satellites.

Fig. 7. A photo of body mounted satellite.

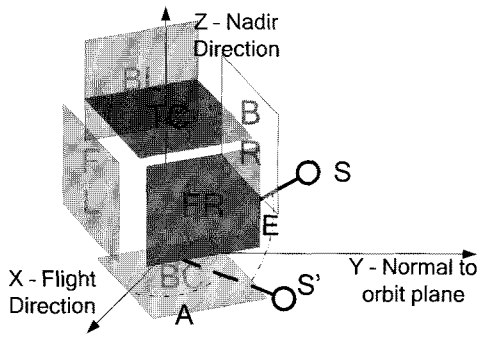

Fig. 8. 3D model of sun sensor.

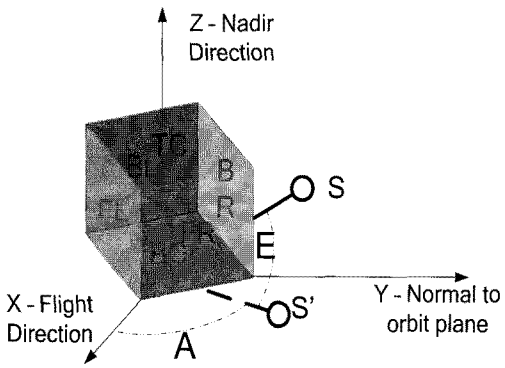

Fig. 9. 3D model of sun sensor.

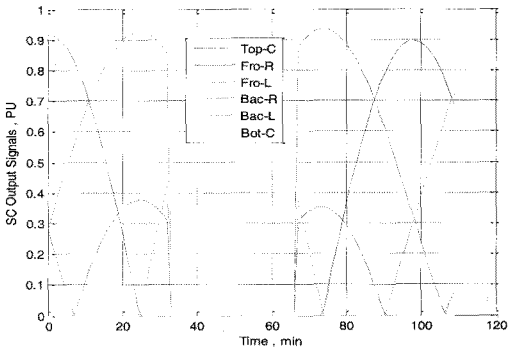

Fig. 10. Solar Cells output signals.

Equations (14) – (19) present the mathematical models of the solar cells (solar arrays) output signal in the orbital coordinate system by means without any perturbation in the X, Y or Z axis. The results are shown in Fig. 10.

The output signals of the solar cells are used to estimate the sun vector in the orbital coordinates. By adding Eq. 13 and Eq. 15, (output signals from the front right and back right solar cells) the Elevation angle E(t) can be calculated. The information about E(t) is available as long as the two solar cells used are illuminated while the overlapping between these two cells is less than the illuminated duration of the orbit. Otherwise, because of the rotation of the satellite in its orbit, the solar cells get shadowed by the satellite body or by the cells themselves although the satellite is still present in the daylight. To solve this problem, an intelligent routine is added to trace the sun vector; it can be called a sun vector seeker. This routine searches for the illuminated solar cells and uses their output signals to calculate the sun elevation in the orbit plane. The combination of solar cell output signals that are applied to trace the sun elevation angle are as follows:

- Front Right and Back Right solar cell pair, then
- Back Right and Back Left solar cell pair, then
- Front Right and Front Left solar cell pair, and
- Front Right and Back Right solar cell pair again.

By substituting the elevation angle E(t) in either Eq. 14 (output signal of the top solar cell) or Eq. 15 (output signal of the bottom solar cell), the azimuth angle A(t) can be obtained in orbital coordinates also.

6.2 Sun Vector in body frame

The sun vector is required in both orbital coordinates and body coordinates to estimate the satellite attitude, which is our target in this paper. To get the sun vector in the body coordinates, we have to apply the transformation matrix of Φ, θ and φ shown in Eq. 8 to the sun vector in orbital coordinates.

Three values for both E(t) and A(t) are obtained in the developed software: values of E(t) and A(t) in orbital coordinates, calculated values of E(t) and A(t) in body coordinates and measured values of E(t) and A(t) in body coordinates. They are obtained depending on the output signals from the solar cells and the application of the intelligent routine for sun vector seeking. The results are shown in Fig. 11 and Fig. 12.

Fig. 13 and Fig. 14 show the output signals from the six solar cells without and with perturbations in Φ, θ and ψ angles.

From the simulation results, it can clearly be seen that the amplitudes and angles of both sun elevation and azimuth are quite different depending on the different values of the perturbation angles; Φ, θ and ψ. Also, the results confirm that the values of the sun elevation and azimuth in orbital coordinates and the calculated and measured one's in body coordinates coincide. This data is presented as a validation face or test point for the proposed model of the coarse sun sensor and the developed software program of calculations and simulations.

6.3 Accuracy of the Proposed Analog Sun Sensor

The results presented in figures 11-16 show that range of both sun elevation and sun azimuth angles varies from $0-\pi/2$ and $0-2\pi$ respectively. The resolution of the measured analog values depends strongly on the resolution of the analog to digital converter in the attitude determination process controller. Table 1 presents the accomplished resolution as a function of the A/D resolution. Some of the sun sensors, even digital ones introduce 0.1^0 as a sensor resolution. In case that analog sensors use a higher resolution A/D's, a better sensor resolution can be achieved. It is recommended to use A/D converters with 12 bits or higher.

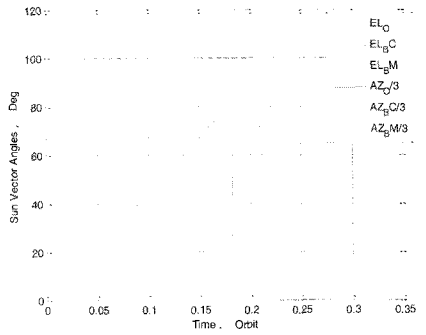

Fig. 11. Sun Vector without Perturbation.

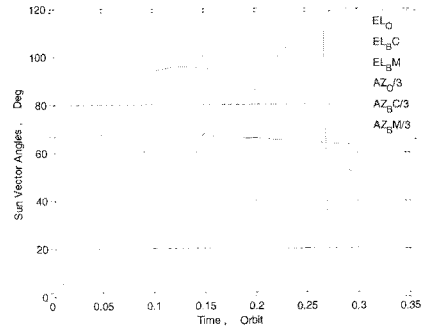

Fig. 12. Sun Vector with Perturbation: Φ =10, θ = -20, ψ =10.

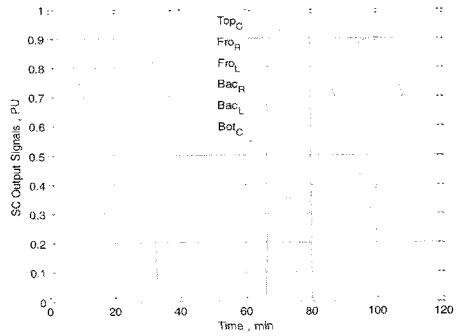

Fig. 13 Solar Cells Output Signals without Perturbation.

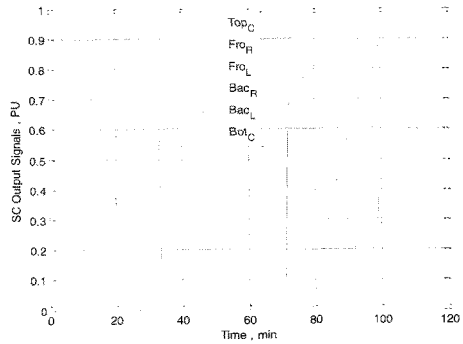

Fig. 14. Solar Cells Output Signals with Perturbation: Φ =10, θ = -20, ψ =10.

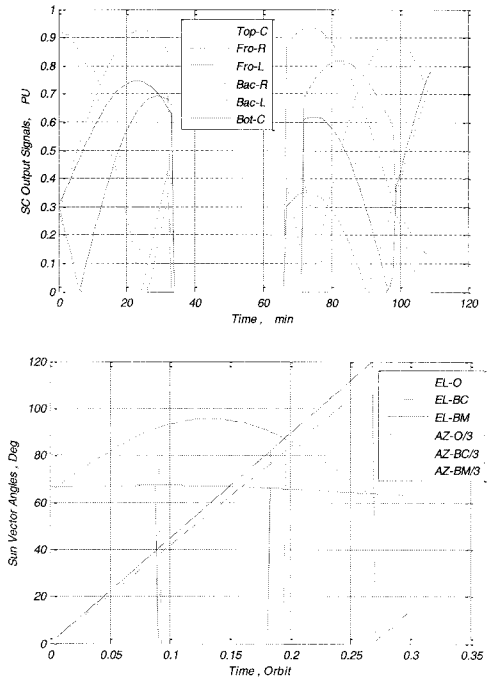

Fig. 15. Simulation results without perturbations, the colored curves as shown in legend and with perturbations $\Phi = 10^0$, $\theta = -20^0$ and $\psi = 10^0$, other six curves in each diagram

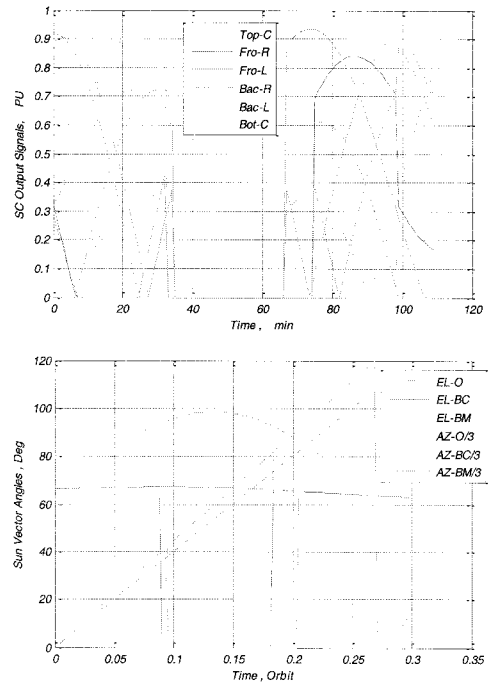

Fig. 16. Simulation results without perturbations, the colored curves as shown in legend and with perturbations $\Phi = 5^0$, $\theta = -25^0$ and $\psi = 13^0$, other six curves in each diagram.

The shadowing or dazzling problems that are mentioned by [1] rarely happened and can be solved by implementing a subroutine to predict and compensate for the effect of this phenomena if it happens.

Table1. Analog Sun Sensor Resolution.

A/D number of bits	Resolution in degrees	
10 bits	0.3515625	0° : 21': 5.625"
12 bits	0.087890625	0° : 5' : 16.406"
14 bits	0.02197265625	0° : 1' : 19.101"
16 bits	0.0054931640625	0° : 0' : 19.775"

7. Spacecraft Attitude Determination

The attitude of a rigid body is defined as the orientation of a fixed body frame with respect to a reference frame [13]. One of the most useful mathematical relations that solves the attitude problem is the attitude matrix or the direction cosine matrix. The direction cosine matrix is a coordinate transformation that maps vectors from the reference frame to the body frame.

In the attitude estimation problem, directions in the body frame to fixed points with known directions in the reference frame are measured. The directions in the body frame are transformed into the known reference directions by pre-multiplying by the rotation matrix defining the attitude of the rigid body. The rotation matrix can be estimated by minimizing an error between the transformed measured directions and the known reference directions [14].

There are many methods that can be used for spacecraft attitude determination. One of these methods is the algebraic method [3, 15-17]. In the algebraic method, the direction cosine matrix is determined directly from two vectors observations without restoring them to any angular representation.

Consider two vectors $\hat{u}, \hat{v}$ and define an orthogonal coordinate system with the basis vector.

$$\text{Let } \hat{q} = \hat{u} \tag{20}$$

$$\text{Construct } \hat{r}, \quad \hat{r} = \frac{\hat{u} \times \hat{v}}{|\hat{u} \times \hat{v}|} \tag{21}$$

At a given time, two measured vectors in the spacecraft body coordinates $\hat{u}_B, \hat{v}_B$, determine the body matrix

$$M_B = (\hat{q}_B, \hat{r}_B, \hat{S}_B \quad (23)$$

The reference matrix is constructed from $\hat{u}_R$, $\hat{v}_R$ by

$$M_R = (\hat{q}_R, \hat{r}_R, \hat{S}_R) \quad (24)$$
$$\therefore D_c = M_B M_R^{-1}$$

Where,

Dc is the direction cosine matrix,

$$D_c = M_B M_R^{-1} \quad (25)$$

Since the reference matrix is the vectors in the orbital coordinates, the direction matrix will be the same as R_b^o (Eq.8)

Hence, the direction cosine matrix Dc is calculated, so the spacecraft attitude is totally determined. The reference matrix is constructed from the Sun vector in the orbital coordinate system (OCS) "$\hat{S}_o$", and the Earth vector in the OCS "$\hat{N}_o$", and from these two vectors the reference matrix M_R can be easily determined. The body matrix is constructed from the Sun vector in the body coordinate system (BCS) "$\hat{S}_B$", and the Earth vector in the BCS "$\hat{N}_B$", and from these two vectors the body matrix M_B can be easily determined.

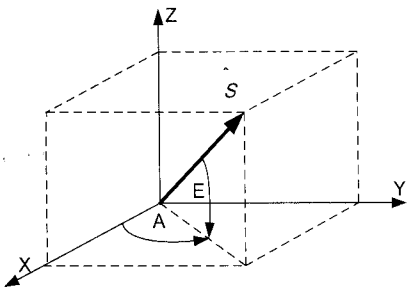

Fig. 17. The Sun vector representation using angles E and A.

7.1 The Sun Sensor Model

The sun vector can be expressed either in orbital or in body coordinates as a function of the sun elevation and azimuth angles as shown in Fig. 17 and Eq. (26).

$$\hat{S} = \begin{bmatrix} \cos A . \sin E \\ \sin A . \sin E \\ \cos E \end{bmatrix} \quad (26)$$

The Sun vector in the OCS "$\hat{S}_o$" is found from the Sun propagator, when representing a spacecraft attitude change the Sun vector in the BCS "$\hat{S}_B$", will change as the output from the solar panels for the spacecraft axes (angles E and A in equation 26) also changes, and, hence, the deviation of $\hat{S}_B$ from $\hat{S}_o$ will appear (when the spacecraft attitude angles equal zero the vectors $\hat{S}_B$ and $\hat{S}_o$ are coincident).

The Earth vector in the OCS "$\hat{N}_o$" equals the vector which corresponds to the Nadir, while the Earth vector in the BCS "$\hat{N}_B$" is the output of the Earth sensor in which, when a spacecraft attitude change is found, the deviation of $\hat{N}_B$ from $\hat{N}_o$ will appear.

7.2 The Earth Sensor Model

The Earth Sensor model can be developed by calculating the projection of the Earth vector in the OCS "$\hat{N}_o$" in the Earth Sensor sensing axis (which is transformed from the BCS through its multiplication by the mounting transformation matrix). This can be done in the following steps:

Step 1. Input the Earth vector in the OCS "$\hat{N}_o$";

Step 2. Transfer the Earth vector in the OCS "$\hat{N}_o$" to BCS "$\hat{N}_B$" by determining the spacecraft attitude angles between the BCS and the OCS, (from it calculate the direction cosine matrix M = Eq. (8).

$$\hat{N}_B = M\,\hat{N}_0 \tag{27}$$

Step 3. Add the alignment and orthogonality errors (i.e. calculate the Earth vector in the Earth sensor axis)

$$\hat{N}_{OA} = C_{OA} N_B \tag{28}$$

Where: $C_{OA} = C_O C_A$ is the resultant transformation matrix of the orthogonality and alignment errors matrices, respectively.

Step 4. Add the measurement errors (random and due to temperature) to the MM measurement

$$\hat{N}_{BO} = \hat{N}_{AO} + \zeta_{T,R} \tag{29}$$

Where,

$\zeta_{T,R}$ is the random measurement error.

7.3 Spacecraft Attitude Determination Cases

The spacecraft attitude determination is valid while the Sun and Earth sensors are operating. This means that the spacecraft eclipse periods will affect the Sun sensor readings. For a LEO spacecraft, the eclipse periods are about one third of the orbital rate. In this case, the Sun and Earth vectors in BCS are coincident as shown in Fig. 18 (case 4). The Sun sensor reading is not available during an eclipse and the yaw data is missing in this case. Observers can substitute for the lack of the yaw measurement in this case depending on the gyros and Earth sensor measurements as in [18], but we are not concerned with this case.

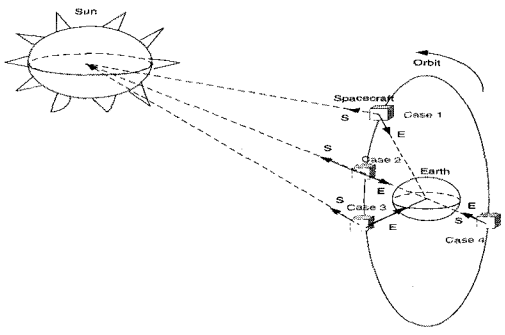

Fig. 18. Represents the spacecraft while orbiting, and shows the Sun and Earth vectors in the spacecraft frame(BCS).

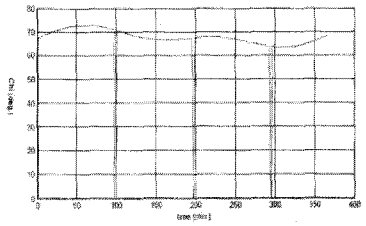

Fig. 19. The angle between the Sun and Earth vectors (Chi).

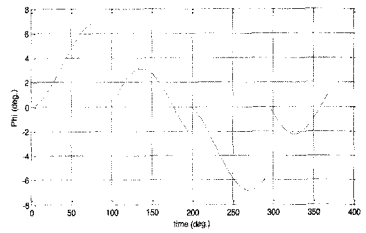

Fig. 20. The spacecraft roll angle (phi).

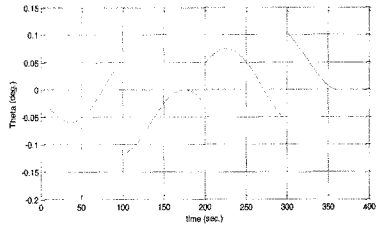

Fig. 21. The spacecraft pitch angle (theta).

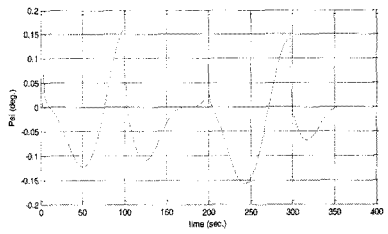

Fig. 22. The spacecraft pitch angle (theta).

The case in which the Sun and Earth sensors are operating in the two thirds of the orbital rate is discussed here. In this case, there are regions in which the Sun and Earth vectors in the BCS are aligned where the spacecraft attitude measurement is missing. The case during, before, and after this alignment are shown in Fig.18 (case 1, 2 and 3). Note: case 2 in Fig. 18 represents the spacecraft attitude complete loss.

The spacecraft attitude determination algorithm fails to provide the attitude. This can be solved again by observers that can provide information about the spacecraft attitude in this case for a very small period.

In the following figures, the angle between the Sun and Earth vectors (Chi) in BCS, the spacecraft attitude angles (roll, pitch and yaw) are plotted for the case when the spacecraft are in the Nadir pointing position.

In Fig. 19 the angle between the Sun and Earth vectors (Chi) is depicted. The angle value is between 68 and 72 degrees. In the case of a spacecraft eclipse or having an angle of 180 degrees between the Sun and Earth vectors in the BCS, the Chi angle is equal to zero as shown in the Figure (this appears as a discontinuity in the Chi angle graph).

In Fig. 20 the spacecraft roll angle is depicted. The angle value is between -6 and 6 degrees. The error here for the roll angle is moderately large. In the case of Chi angle discontinuities, the roll angle is not determined as the attitude algorithm fails, and there is no information about the roll angle as shown in Fig. 20.

In Fig. 21 the spacecraft pitch angle is depicted. The angle value is between -0.12 and 0.12 degrees. The error here is less than that of the roll angle. In the case of Chi angle discontinuities, the pitch angle is not determined as the attitude algorithm fails, and there is no information about the spacecraft pitch angle as shown in the figure.

In Fig. 22 the spacecraft yaw angle is depicted. The angle value is between -0.13 and 0.13 degrees. The error here is similar to the pitch angle error and is less than that of the roll angle. In the case of Chi angle discontinuities, the yaw angle is not determined as the attitude algorithm fails, and there is no information about the spacecraft yaw angle as shown in the figure.

8. Conclusions

A coarse analog sun sensor based on solar cell applications is presented in this paper. The mathematical model of the generated energy from each solar array side in a cube-shaped satellite is deduced. A software program is developed using MatLab to simulate a satellite in orbit and calculate the output power waveform from each solar module (solar cell). The results show the daylight and eclipse period for each solar array and help the developer to create an intelligent subroutine to make a combination with an appropriate solar array together to calculate the sun elevation and azimuth. The calculated angles that will be used to estimate the sun vector in both orbitals and the body coordinate to estimate the satellite attitude are examined by applying a known disturbance to the direction matrix and calculating the values of these angles again by measuring the output signals from the solar cells. The results confirm that the developed model is accurate and the feedback error approximately zero.

Sun and Earth sensors are used for attitude determination and the models of both are presented as well as the MatLab program developed for calculations. The developed coarse sun sensor can provide a competitive resolution compared to the expensive and limited lifetime digital ones. An analog sun sensor is cheap, reliable and can be applied alone as a sun sensor or combined with digital ones as a backup or online redundancy to enhance the attitude determination subsystem and, hence, the overall reliability.

The spacecraft attitude determination in this paper is investigated when the spacecraft BCS is coincident with the OCS. The error which appears for the spacecraft roll angle is much large than that of the pitch and yaw angles. More investigations should be done in order to enhance the measurements using this coarse Sun sensor to attain better accuracy at low cost.

References

[1] Yonatan Winetraub et.al, "Attitude Determination Advanced Sun Sensors for Pico-satellites," *17th European Union Contest for Young Scientists*, Moscow, Bauman Univ., Sept., 2005.

[2] Sensors for Spacecraft Applications, www.tsgc.utexas.edu/achieve/subsystems/sensors.pdf.

[3] Ralph D Lorenz, Flight *and attitude dynamics measurements of an instrumented Frisbee*, IOP Publishing Ltd, 2005.

[4] J. Wertz, *Spacecraft Attitude Determination & Control*, Microcosm inc., 1978.

[5] Kristin L. Makovec, Andrew J. Turner and Christopher D. Hall, "Design and Implementation of a Nanosatellite Attitude Determination and Control System", AAS 01-311.

[6] Jo Ryeong Yim, John L. Crassidis and John L. Junkins, "Autonomous Orbit Navigation of Interplantary Spacecraft," *American Institute of Aeronautics and Astronautics Paper*, AIAA-2000-3936.

[7] Michael Swartwout, Tanya Olsen, Christopher Kitts, "THE Omni-Directional Differential Sun Sensor," *in proc. of 31st Annual International Telemetry Conference: Reengineering*

Telemetry, 1995. ssdl.stanford.edu/ssdl/images/stories/papers/1995/ssdl9501.pdf

[8] M. Ferrante, M. Povia, L. Di Ciolo,A. Ortenzi, M. Petrozzi, *IRECINN ano-satellite communication system and ground segment*, Acta Astronautica, 2005.

[9] Hank Heidtl, Jordi Puig-Suari2, Augustus S. Moore3, Shinichi Nakasuka4, and Robert J. Twiggs5, "CubeSat: A new Generation of Picosatellite for Education and Industry Low-Cost Space Experimentation", *in proc. of 4th Annual AIAA/USU Conference on Small Satellites*, 2001.

[10] Brian M. Menges, Carlos A. Guadiamos, and Emily K. Lewis, "Dynamic Modeling of MicroSatellite Spartnik's Attitude," http://www.engr.sjsu.edu/spartnik/pdf/adacpaper.pdf.

[11] Bernt Ove Sunde, "Sensor modeling and attitude determination for micro-satellite," *M.Sc Thesis, Departement of Engineering Cybernetics*, Norwegian University of Science and Technology (NTNU), June, 2005.

[12] M. Zahran, "In Orbit Performance of LEO Satellite Electrical Power Subsystem - SW Package for Modelling and Simulation Based on MatLab.7 GUI," *Journal of WSEAS Transactions on Power Systems*, Vol. 1, No. 5, 2006.

[13] Chbotov, A. V., *Spacecraft Attitude Dynamics and Control*, OrbitTM A Foundation SERIES, 1991.

[14] T. Lee, A. Sanyal, M. Leok, and N. McClamroch, "Deterministic Global Attitude Estimation," *in Proc. of the 45th IEEE Conference on Decision & Control*, 2006.

[15] Sidi, M., *Spacecraft Dynamics & Control*, Cambridge Univ. press, 1997.

[16] Crassidis, J. L. and Markley, F. L., Y. Cheng, "Survey of Nonlinear Attitude Estimation Methods," *Journal of Guidance, Control, and Dynamics*, Vol. 30, No.1, 2007.

[17] D. Choukroun, I. Y. Bar-Itzhack, and Y. Oshman, "Optimal-Request Algorithm for Attitude Determination," *Journal of Guidance, Control, and Dynamics*, Vol. 27, No. 3, 2004.

[18] M. Aly, "Observers for Spacecraft Attitude Estimation," *M.Sc. thesis*, Faculty of Engineering, Cairo University-Giza-Egypt, December 2005.

[19] Jeong-Man Han, Byung-Hwan, Jeong Jae-Seok Gho, Gyu-Ha Choe, "Analysis of PWM Converter for V-I Output Characteristics of Solar Cell," *Journal of Power Electronics*, Vol. 3, No. 1, pp.62-67, 2003.

[20] M. Zahran, M. Okasha, Galina A. Ivanova, "Assessment of Earth Remote Sensing Microsatellite Power Subsystem Capability during Detumbling and Nominal Modes," *Journal of Power Electronics*, Vol. 6, No. 1, pp.18-28, 2006.

[21] M. Zahran, S. Tawfik, Gennady Dyakov, "L.E.O. Satellite Power Subsystem Reliability Analysis," *Journal of Power Electronics*, Vol. 6, No. 2, pp.104-113, 2006.

[22] Sheldon S. Williamson, S. Chowdary Rimmalapudi, Ali Emadi, "Electrical Modeling of Renewable Energy Sources and Energy Storage Devices," *Journal of Power Electronics*, Vol. 4, No. 2, pp.117-126, 2004.

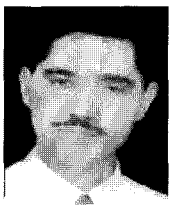

Mohamed Bayoumy A. Zahran was born in Egypt in 1963, received his B.Sc from Kima High Institute of Technology in 1987, his M.Sc in 1993 and his Ph.D. in 1999 from Cairo University, Faculty of Engineering, Electrical Power and Machines Dept. He is an Associate Professor Researcher in the Electronics Research Institute, Photovoltaic Cells Dept. His experience is mainly in the fields of renewable energy sources, systems design, and management and control. He has been employed full-time by the National Authority for Remote Sensing and Space Science (NARSS), Space Division, since 2002, as a System Engineer of the MisrSat-2 Project and a Satellite Power Subsystem Designer. He has been serving as a Participant Professor at Jizan University Faculty of Engineering, Electrical Engineering Department, Kingdom of Saudi Arabia, since 1st Oct., 2008.

Mohamed M. Aly received the B.SC. in Electrical Engineering (control and measurements) from Benha Higher Institute of Technology, Benha Univ.-Egypt in '99, and the M.SC. in Electrical Engineering (Automatic Control) from the Faculty of Engineering, Cairo Univ.-Egypt in '05. He worked on the EgyptSat-1 satellite project (a contract between the National Authority for Remote Sensing and Space Sciences-Egypt and Yuzhnoye S.D.O.-Ukraine) as a spacecraft Attitude Determination and Control Subsystem (ADCS) hardware engineer from 2002 to 2008. Currently, he is a research assistant and a PhD student at the Aerospace Engineering Dept., Old Dominion Univ.-Norfolk, VA, USA.